8 Multiplets in Transition Metal Ions

Robert Eder
Institut für Festkörperphysik
Karlsruhe Institute of Technology

Contents

E. Pavarini, E. Koch, F. Anders, and M. Jarrell
Correlated Electrons: From Models to Materials
Modeling and Simulation Vol. 2
Forschungszentrum Jülich, 2012, ISBN 978-3-89336-796-2
http://www.cond-mat.de/events/correl12

1 Introduction

Compounds containing $3d$ transition metal – or iron group – ions have been intriguing solid state physicists ever since the emergence of solid state physics as a field of research. In fact, already in the 1930's NiO became the first known example of a correlated insulator in that it was cited by deBoer and Verwey as a counterexample to the then newly invented Bloch theory of electron bands in solids [1]. During the last 25 years $3d$ transition metal compounds have become one of the central fields of solid state physics, following the discovery of the cuprate superconductors, the colossal magnetoresistance phenomenon in the manganites and, most recently, the iron-pnictide superconductors.

It was conjectured early on that the reason for the special behaviour of these compounds is the strong Coulomb interaction between electrons in the partially filled $3d$ shells of the iron group elements. These $3d$ wave functions are orthogonal to those of the inner-shells – $1s$, $2s$ and $2p$ – solely due to their angular part $Y_{2,m}(\Theta, \phi)$. Their radial part $R_{3,2}(r)$ thus is not pushed out to regions far from the nucleus by the requirement to be orthogonal to the inner shell wave functions and therefore is concentrated close to the nucleus (the situation is exactly the same for the $4f$ wave functions in the Rare Earth elements). Any two electrons in the $3d$ shell thus are forced to be close to each other on average so that their mutual Coulomb repulsion is strong (the Coulomb repulsion between two $3d$ electrons is weak, however, when compared to the Coulomb force due to the nucleus and the inner shells so that the electrons *have to* stay close to one another!). For clarity we also mention that the Coulomb repulsion between two electrons in the inner shells of most heavier elements is of course much stronger than between the $3d$ electrons of the iron group elements. This, however, is irrelevant because these inner shells are several 100 - 1000 eV below the Fermi energy so that they are simply completely filled. The $3d$-orbitals in the iron group elements or the $4f$-orbitals in the Rare Earths on the other hand participate in the bands at the Fermi level so that the strong Coulomb interaction in these orbitals directly influences the conduction electrons. This is why the Coulomb repulsion in these shells dominates the physical properties of these compounds and gives rise to such a wide variety of interesting phenomena. Let us therefore discuss the Coulomb interaction in a partially filled atomic shell in more detail.

2 Multiplets of a free ion

2.1 General considerations

For definiteness we consider NiO. The atomic electron configurations are [Ar]$3d^8 4s^2$ for Nickel and [He]$2s^2 2p^4$ for Oxygen. In a purely ionic picture the oxgen atom will want to fill its $2p$ shell and become O^{2-}, rendering Ni to be Ni^{2+} with electron configuration [Ar]$3d^8$. Accordingly let us first consider a Ni^{2+} ion *in vacuum*. It is a standard exercise in textbooks of atomic physics to show that the d^8 configuration, which is equivalent to d^2, has the following multiplets: ${}^3F$, ${}^3P$, ${}^1G$, ${}^1D$ and ${}^1S$. The energies of these multiplets differ and can be observed experimentally, e.g.,

in the spectrum of Ni vapor. The first two Hund's rules state that the multiplet with the lowest energy, i.e., the ground state of the Ni^{2+} ion, is ${}^3F$. Then we may ask: what is the physical mechanism that leads to the multiplet splitting and makes ${}^3F$ the ground state? The answer is that it is the Coulomb repulsion between $3d$ electrons which splits the multiplets energetically and enforces the first two Hund's rules. When being asked for the energy of the d^n configuration one might give be tempted to give the following answer:

$$E[d^n] \approx n \cdot \epsilon_d + U \cdot \frac{n(n-1)}{2}.$$

The first term, where ϵ_d is the energy of the d-orbital, is the single-particle energy. The second term obviously counts the number of electron pairs and multiplies them by the parameter U which accordingly has the meaning of an average Coulomb repulsion energy between two electrons. For a non-degenerate orbital, instead of the five-fold degenerate d-orbital, n can take only the values 0, 1 and 2, with corresponding Coulomb energies 0, 0 and U. In this case the second term therefore reduces to the expression $Un_\uparrow n_\downarrow$ familiar from the Hubbard or Anderson model.

In a degenerate situation, however, the Coulomb interaction between electrons has additional aspects. Let us first consider a classical picture where the electrons are taken as charged mass points orbiting around the nucleus. In this case the Colomb force $\boldsymbol{F}_{ij}$ acting on electron i due to electron j in general is not parallel to the position vector $\boldsymbol{r}_i$ of electron i and thus exerts a nonvanishing torque $\boldsymbol{\tau}_{ij} = \boldsymbol{r}_i \times \boldsymbol{F}_{ij}$. This means that the angular momentum of any given electron changes constantly but since $\boldsymbol{F}_{ij} = -\boldsymbol{F}_{ji} = f(|\boldsymbol{r}_i - \boldsymbol{r}_j|)\ (\boldsymbol{r}_i - \boldsymbol{r}_j)$ it is easy to see that $\boldsymbol{\tau}_{ij} = -\boldsymbol{\tau}_{ji}$ so that the two electrons i and j merely 'exchange angular momentum' and the total angular momentum is conserved. The quantum mechanical version of this exchange of angular momentum is shown in Fig. 1: The 8 d-electrons are initially distributed over the 5 d-orbitals which are labeled by the m-value in the angular part of their wave functions, $Y_{2,m}(\Theta, \phi)$. Then, two electrons scatter from each other due to their Coulomb interaction and after the scattering find themselves in orbitals with a different m-value. The sum over the m-values of the occupied orbitals, which gives the z-component of the total orbital angular momentum L^z, must remain constant during the scattering process so that the two scattering electrons move

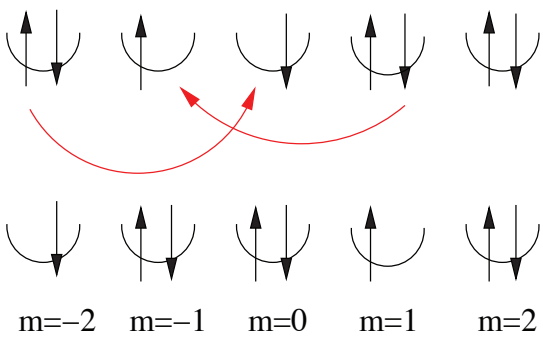

Fig. 1: *A scattering process between two electrons in a partly filled d-shell.*

along the 'm-ladder' in opposite direction and by an equal number of steps. The single particle energy of the electrons, which is $8\epsilon_d$ in Fig. 1, is unchanged by the scattering. This means that scattering processes of the type shown in Fig. 1 connect all states with a given z-component of the total spin and orbital angular momentum and all of these states are degenerate with respect to their single particle energy. If we think of an unperturbed Hamiltonian H_0 which consists of the single particle energies of the various levels and consider the Coulomb interaction between the $3d$ electrons as perturbation H_1 we have exactly the situation of degenerate first order perturbation theory. The textbook procedure then is to set up the secular determinant, i.e., the matrix $\langle\mu|H_1|\nu\rangle$ where $|\mu\rangle$ and $|\nu\rangle$ run over the set of degenerate eigenstates of H_0, and diagonalize this.

To formulate this in a more quantitative fashion we first introduce Fermionic creation (and annihilation) operators $c^\dagger_{n,l,m,\sigma}$ which create an electron with z-component of spin σ in the orbital with principal quantum number n, orbital angular momentum l, and z-component of orbital angular momentum m. In the following we will often contract (n, l, m, σ) to the 'compound index' ν for brevity, so that e.g. $c^\dagger_{\nu_i} = c^\dagger_{n_i,l_i,m_i,\sigma_i}$. In our case the degenerate states $|\nu\rangle$ can be written as

$$|\nu\rangle = |\nu_1, \nu_2 \ldots \nu_n\rangle = c^\dagger_{\nu_1} c^\dagger_{\nu_2} \ldots c^\dagger_{\nu_n} |0\rangle. \tag{1}$$

In the case of a partly filled $3d$-shell all $n_i = 3$ and all $l_i = 2$ identically, so that these two indices could be omitted, but we will keep them for the sake of later generalizations. In writing the basis states as in (1) we need to specify an ordering convention for the creation operators on the right hand side. For example, only states are taken into account where $m_1 \leq m_2 \leq m_3 \cdots \leq m_n$. Moreover, if two m_i are equal the $c^\dagger_{m_i\downarrow}$-operator is assumed to be to the left of the $c^\dagger_{m_i\uparrow}$-operator. If we adopt this convention, every possible state obtained by distributing the n electrons over the $2(2l+1)$ spin-orbitals is included exactly once in the basis. If the n_i and l_i were to take different values we could generalize this by demanding that the (n_i, l_i, m_i)-triples be ordered lexicographically. As will be seen below, strict application of an ordering convention for the Fermi operators is necessary to determine the correct Fermi signs for the matrix elements. In second quantization the Coulomb Hamiltonian H_1 then reads (in atomic units)

$$\begin{aligned} H_1 &= \frac{1}{2} \sum_{i,j,k,l} V(\nu_i, \nu_j, \nu_k, \nu_l)\; c^\dagger_{\nu_i} c^\dagger_{\nu_j} c_{\nu_k} c_{\nu_l}, \\ V(\nu_1, \nu_2, \nu_3, \nu_4) &= \int dx \int dx'\; \psi^*_{\nu_1}(x)\; \psi^*_{\nu_2}(x')\; V_c(x, x')\; \psi_{\nu_4}(x)\; \psi_{\nu_3}(x'), \\ V_c(x, x') &= \frac{1}{|\boldsymbol{r} - \boldsymbol{r}'|}. \end{aligned} \tag{2}$$

Here $x = (\boldsymbol{r}, \sigma)$ is the combined position and spin coordinate and V_c is the Coulomb interaction between electrons. Note the factor of $1/2$ in front of H_1 and the correspondence of indices and integration variables $\nu_4 \leftrightarrow x$ and $\nu_3 \leftrightarrow x'$ in the Coulomb matrix element, see textbooks of many-particle physics such as Fetter-Walecka [2]. In the next paragraph we will calculate the matrix elements $V(\nu_1, \nu_2, \nu_3, \nu_4)$.

2.2 Calculation of the Coulomb matrix elements

First, we use the fact that the single-particle basis we are using consists of atomic spin-orbitals so if we parameterize the vector $\boldsymbol{r}$ by its polar coordinates (r, Θ, ϕ) we have

$$\psi_{\nu_i}(x) \;\; = \;\; R_{n_i,l_i}(r)\; Y_{l_i,m_i}(\Theta,\phi)\; \delta_{\sigma,\sigma_i}. \tag{3}$$

The radial wave functions R_{n_i,l_i} are assumed to be real, as is the case for the true radial wave function of bound states in a central potential. Apart from this we do not really specify them. In fact, it would be rather difficult to give a rigorous prescription for their determination. It will turn out, however, that these radial wave functions enter the matrix elements only via a discrete and rather limited set of numbers which are very often obtained by fit to experiment.
In addition to (3), we use the familiar multipole expansion of the Coulomb interaction

$$\frac{1}{|\boldsymbol{r}-\boldsymbol{r}'|} \;\; = \;\; \sum_{k=0}^{\infty} \sum_{m=-k}^{k} Y^*_{k,m}(\Theta',\phi')\; \frac{4\pi}{2k+1}\; \frac{r_<^k}{r_>^{k+1}}\; Y_{k,m}(\Theta,\phi). \tag{4}$$

We now evaluate the matrix element $V(\nu_1,\nu_2,\nu_3,\nu_4)$ and first note that the sum over spin variables simply gives the prefactor $\delta_{\sigma_1,\sigma_4}\;\delta_{\sigma_2,\sigma_3}$. Next we pick one term with given k and m from the multipole expansion (4) and proceed to the integration over the spatial variables (r,Θ,ϕ) and (r',Θ',ϕ'). Let us first consider the angular variables (Θ,ϕ). Obviously these always come as arguments of spherical harmonics and there is one from $\psi^*_{\nu_1}(x)$, i.e., the bra, one from the multipole expansion (4), i.e., H_1, and one from $\psi_{\nu_4}(x)$, i.e., the ket. We thus find a factor of

$$\int_0^{2\pi} d\phi \int_{-1}^{1} dcos(\Theta)\; Y^*_{l_1,m_1}(\Theta,\phi)\; Y_{k,m}(\Theta,\phi)\; Y_{l_4,m_4}(\Theta,\phi) \tag{5}$$

Such a dimensionless integral over three spherical harmonics is called a Gaunt coefficient and can be shown to be proportional to a Clebsch-Gordan coefficient [3,4]. An interesting property can be seen if we note the ϕ-dependence of $Y_{l,m}(\Theta,\phi) = P_{l,m}(\Theta)\; e^{im\phi}$ whence we find that the Gaunt coefficient (5) is different from zero only if $m_1 = m_4 + m$. Moreover, the Θ-dependent factors $P_{l,m}(\Theta)$ are all real [3,4], so that all nonvanishing Gaunt coefficients are real. In exactly the same way the integration over (Θ',ϕ') gives

$$\int_0^{2\pi} d\phi' \int_{-1}^{1} dcos(\Theta')\; Y^*_{l_2,m_2}(\Theta',\phi')\; Y^*_{k,m}(\Theta',\phi')\; Y_{l_3,m_3}(\Theta',\phi'), \tag{6}$$

which by similar arguments is different from zero only if $m_2 + m = m_3$. Since (5) and (6) must be different from zero for the same m in order to obtain a nonvanishing contribution we must have $m_1 + m_2 = m_3 + m_4$. This is simply the condition, stated already above, that L^z be conserved.
It remains to do the integral over the two radial variables r and r'. These two integrations cannot be disentangled and we find a last factor

$$R^k(n_1l_1,n_2l_2,n_3l_3,n_4l_4) = \int_0^{\infty} dr\, r^2 \int_0^{\infty} dr' r'^2\; R_{n_1l_1}(r) R_{n_2l_2}(r')\; \frac{r_<^k}{r_>^{k+1}}\; R_{n_4l_4}(r) R^l_{n_3l_3}(r'). \tag{7}$$

These integrals, which have the dimension of energy, are labeled by the multipole index k and in the present case of Coulomb scattering within a d-shell the number of relevant multipole orders is severely limited by the properties of the Gaunt coefficients. First, since the latter are proportional to Clebsch-Gordan coefficients the three l-values appearing in them have to obey the so-called *triangular condition* [5] whence $k \leq \min(|l_1 + l_4|, |l_2 + l_3|)$. For a d-shell where $l_i = 2$ it follows that $k \leq 4$. Second, the parity of the spherical harmonic Y_{lm} is $(-1)^l$, i.e., even for the case $l_i = 2$. For integrals such as (5) or (6) to be different from zero the spherical hamonic Y_{km} from the multipole expansion must have even parity, too, so that for Coulomb scattering within a d-shell only R^0, R^2 and R^4 are relevant. This shows that the sloppy definition of the wave function $R_{n_i,l}(r)$ is not a real problem – details of this wave function are irrelevant anyway. In a way, these three parameters may be viewed as a generalization of the Hubbard-U in that R^k is something like the 'the Hubbard-U for k-pole interaction'.
Next, we introduce the following short notation for nonvanishing Gaunt coefficients

$$c^k(lm;l'm') \;=\; \sqrt{\frac{4\pi}{2k+1}} \int_0^{2\pi} d\phi \int_{-1}^{1} dcos(\Theta)\; Y^*_{lm}(\Theta,\phi)\; Y_{k,m-m'}(\Theta,\phi)\; Y_{l',m'}(\Theta,\phi). \tag{8}$$

These coefficients are tabulated in Appendix 20a of the textbook by Slater [3] or Table 4.4 of the textbook by Griffith [4], see also the Appendix of the present note. Using this notation we can write the complete Coulomb matrix element as

$$\begin{aligned} V(\nu_1,\nu_2,\nu_3,\nu_4) \;=\; & \delta_{\sigma_1,\sigma_4}\,\delta_{\sigma_2,\sigma_3}\,\delta_{m_1+m_2,m_3+m_4} \sum_{k=0}^{\infty} c^k(l_1m_1;l_4m_4)\; c^k(l_3m_3;l_2m_2) \\ & R^k(n_1l_1,n_2l_2,n_3l_3,n_4l_4). \end{aligned} \tag{9}$$

To conclude this paragraph we discuss *particle-hole symmetry*. This phrase expresses the fact that in a shell with angular momentum l the configurations with n electrons and $2(2l+1)-n$ electrons, i.e., n holes, have the same multiplets and that the energies of the multiplets are the same up to an overall additive constant. We consider the following transformation:

$$\begin{aligned} |0\rangle \;&\rightarrow\; |0'\rangle = c^\dagger_{l,-l,\downarrow} c^\dagger_{l,-l,\uparrow} c^\dagger_{l,-l+1,\downarrow} c^\dagger_{l,-l+1,\uparrow} \ldots c^\dagger_{l,l,\downarrow} c^\dagger_{l,l,\uparrow} |0\rangle \\ c^\dagger_\nu \;&\rightarrow\; h_\nu, \\ c_\nu \;&\rightarrow\; h^\dagger_\nu. \end{aligned} \tag{10}$$

This transformation replaces the empty state $|0\rangle$ by the filled shell $|0'\rangle$ and the electron creation/annihilation operators $c^\dagger/c$ by *hole* annihilation/creation operators $h/h^\dagger$. We will now show that the Hamiltonian H_1, when expressed in terms of the hole operators, up to a constant, has the same form as the original Hamiltonian. Once this is shown, we can define basis states $h^\dagger_{\nu_1} \ldots h^\dagger_{\nu_n}|0'\rangle$ which have n holes in the filled shell but have exactly the same matrix elements between them as states of n electrons.
To show the equivalence we assume that in the Coulomb Hamiltonian (2) all Fermion c-operators are replaced by h-operators according (10). Then, in each term we can permute the Fermion

operators according to

$$h_{\nu_1} h_{\nu_2} h^\dagger_{\nu_3} h^\dagger_{\nu_4} = h^\dagger_{\nu_4} h^\dagger_{\nu_3} h_{\nu_2} h_{\nu_1} + \delta_{\nu_2\nu_3} h_{\nu_1} h^\dagger_{\nu_4} - \delta_{\nu_1\nu_3} h_{\nu_2} h^\dagger_{\nu_4} + \delta_{\nu_2\nu_4} h^\dagger_{\nu_3} h_{\nu_1} - \delta_{\nu_1\nu_4} h^\dagger_{\nu_3} h_{\nu_2}$$

where the terms quadratic in h-operators originate from anticommutations. The quartic terms now have the original form, but with the replacement $c \to h$ and

$$V(\nu_4, \nu_3, \nu_2, \nu_1) \to V(\nu_1, \nu_2, \nu_3, \nu_4).$$

As can be seen from (2), however, this replacement is equivalent to complex conjugation of the matrix elements, and since the matrix elements V are real – see (9) – the quartic terms of the Hamiltonian expressed in terms of the hole-operators have the same form as the original Hamiltonian in terms of electron operators.
As for the quadratic terms it can be shown by a somewhat lengthy calculation, see for example Chapter 14 of Slaters textbook [3], that they can be brought to the form $C_1 n + C_2$ with real constants C_1 and C_2 and n the number of holes. For fixed n this is just a constant shift.
This theorem shows that the energies of the d^8 multiplets are, up to an additive constant, identical to those of the d^2 multiplets. Some terms in the Hamiltonian which will be discussed later do not remain invariant under the particle-hole transformation but change sign.

2.3 Solution of the Coulomb problem by exact diagonalization

We now describe how the problem of the partly filled $3d$-shell can be solved numerically, using the method of exact diagonalization. As already noted this may also be viewed as first order degenerate perturbation theory with respect to the Coulomb interaction between the electrons within a given shell. Our basis states (1) obviously correspond to all possible ways of distributing n electrons over the 10 spin-orbitals of the $3d$-shell (two spin directions for each $m \in \{-2, -1 \ldots 2\}$). As shown in Fig. 2 we can code each of these basis states by an integer $0 \leq i \leq 2^{10}$. If we really use all these integers we are actually treating all states with

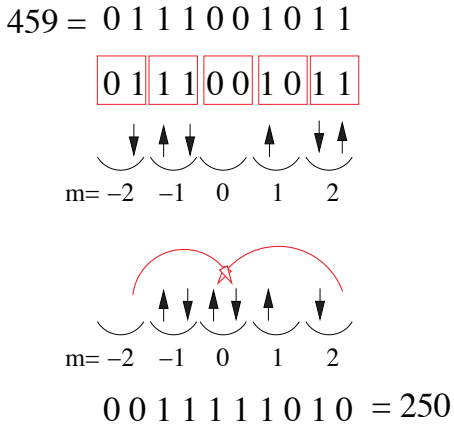

Fig. 2: *The coding of basis states by integers and a scattering process.*

$0 \leq n \leq 10$ simultaneously but this will be convenient for latter generalizations. Next, for a given initial state $|\nu_1, \nu_2, \ldots \nu_n\rangle$ we can let the computer search for all possible transitions of the type shown in Fig. 2 and compute the corresponding matrix elements from (9) using, say, the $c^k(lm; l'm')$ copied from Slater's textbook and some given R^0, R^2 and R^4. Let us consider the following matrix element

$$\langle 0|c_{\mu_n} \ldots c_{\mu_1}\ V(\lambda_1, \lambda_2, \lambda_3, \lambda_4)\ c^\dagger_{\lambda_1} c^\dagger_{\lambda_2} c_{\lambda_3} c_{\lambda_4}\ c^\dagger_{\nu_1} c^\dagger_{\nu_2} \ldots c^\dagger_{\nu_n}|0\rangle.$$

For this to be nonzero, the operators $c^\dagger_{\lambda_3}$ and $c^\dagger_{\lambda_4}$ must be amongst the $c^\dagger_{\nu_i}$, otherwise the annihilation operators in the Hamiltonian could be commuted to the right where they annihilate $|0\rangle$. In order for these pairs of operators to cancel each other, c_{λ_4} must first be commuted to the position right in front of $c^\dagger_{\lambda_4}$. If this takes n_4 interachanges of Fermion operators we get a Fermi sign of $(-1)^{n_4}$. Bringing next c_{λ_3} right in front of $c^\dagger_{\lambda_3}$ by n_3 interchanges of Fermion operators gives a sign of $(-1)^{n_3}$. Next, the creation operators $c^\dagger_{\lambda_1}$ and $c^\dagger_{\lambda_2}$ have to be commuted to the right to stand at their proper position as required by the ordering convention – see the discussion after (1). If this requires an additional number of Fermion interchanges n_2 for $c^\dagger_{\lambda_2}$ and and n_1 for $c^\dagger_{\lambda_1}$ there is an additional Fermi sign of $(-1)^{n_1+n_2}$. The total matrix element for this transition then is $(-1)^{n_1+n_2+n_3+n_4} V(\lambda_1, \lambda_2, \lambda_3, \lambda_4)$. The correct Fermi sign thereby is crucial for obtaining correct results and must be computed by keeping track of all necessary interchanges of Fermion operators. This is perhaps the trickiest part in implementing the generation of the Hamilton matrix or any other operator as a computer program.

Once the matrix has been set up it can be diagonalized numerically. Thereby it is a good check to evaluate the expectation values of the square of the orbital angular momentum and spin, $\boldsymbol{L}^2$ and $\boldsymbol{S}^2$, which also allow to assign the standard term symbols. The operator of orbital angular momentum can be written down by noting that the only nonvanishing matrix elements of the spin raising/lowering operator are $\langle l, m \pm 1|L^\pm|l, m\rangle = \sqrt{(l \mp m)(l \pm m + 1)}$ [5] whence

$$\begin{aligned} L^z &= \sum_{m=-l}^{l} \sum_{\sigma}\ m\ c^\dagger_{l,m,\sigma} c_{l,m,\sigma}, \\ L^+ &= \sum_{m=-l}^{l-1} \sum_{\sigma}\ \sqrt{(l-m)(l+m+1)}\ c^\dagger_{l,m+1,\sigma} c_{l,m,\sigma}, \end{aligned}$$

and similar for $L^- = (L^+)^+$. If $|\Psi\rangle$ then is a normalized eigenstate, that means a linear combination of basis states like (1), we define $|\Psi_1\rangle = L^z|\Psi\rangle$, $|\Psi_2\rangle = L^+|\Psi\rangle$ and $|\Psi_3\rangle = L^-|\Psi\rangle$ whence $\langle\Psi|\boldsymbol{L}^2|\Psi\rangle = \langle\Psi_1|\Psi_1\rangle + \frac{1}{2}(\langle\Psi_2|\Psi_2\rangle + \langle\Psi_3|\Psi_3\rangle)$. The procedure for $\boldsymbol{S}^2$ is completely analogous. The resulting expectation values $\langle\boldsymbol{L}^2\rangle$ and $\langle\boldsymbol{S}^2\rangle$ first have to assume the proper quantized values $L(L+1)$ and $S(S+1)$ with integer L and half-integer S and secondly have to be the same for *all* eigenfunctions belonging to a given degenerate eigenvalue. This – and the proper level of degeneracy of each eigenvalue – provides a stringent test for the correctness of the program.

Table 1 gives the resulting multiplet energies for d^8 and d^7, the resulting L and S for each multiplet, as well as the degeneracy n. The values of the R^k parameters have been calculated by using Hartree-Fock wave functions for Ni^{2+} and Co^{2+} in (7). The energy of the lowest

E	S	L	n	Term	E	S	L	n	Term
0.0000	1	3	21	^3F	0.0000	3/2	3	28	^4F
1.8420	0	2	5	^1D	1.8000	3/2	1	12	^4P
1.9200	1	1	9	^3P	2.1540	1/2	4	18	^2G
2.7380	0	4	9	^1G	2.7540	1/2	5	22	^2H
13.2440	0	0	1	^1S	2.7540	1/2	1	8	^2P
					3.0545	1/2	2	10	^2D
					4.5540	1/2	3	14	^2F
					9.9774	1/2	2	10	^2D

Table 1: *Energies of the d^8 multiplets calculated with $R^2 = 10.479\ eV$, $R^4 = 7.5726\ eV$ (Left), and energies of the d^7 multiplets calculated with $R^2 = 9.7860\ eV$, $R^4 = 7.0308\ eV$ (Right).*

multiplet is taken as the zero of energy and it turns out that all *energy differences* depend only on R^2 and R^4. Note the increasing complexity of the level schemes with increasing number of holes in the d-shell. Moreover, the multiplets do span a range of several eV. Finally, the Table shows that the ground states indeed comply with the first two of Hund's rules: they have maximum spin and maximum orbital angular momentum for this spin. It can be shown this is indeed always the case as long as one uses Coulomb and exchange integrals with the correct, i.e. positive, sign [3, 4].

2.4 Special case: Diagonal matrix elements

As will become apparent later, the diagonal elements $\langle\nu|H_1|\nu\rangle$ are of particular importance, so we give explicit expressions for them. We have seen that in a matrix element of H_1 $n-2$ creation operators in the ket $|\nu\rangle = |\nu_1, \nu_2, \ldots \nu_n\rangle$ must be simply cancelled by their Hermitean conjugate in the bra $\langle\nu|$ without ever 'touching' the Hamiltonian. We may then think of the remaining two Fermion operators, which are the ones which *are* paired with Fermion operators in the Hamiltonian, as having been commuted to the first and second position in the ket. This will give uns a Fermi sign, but in a diagonal matrix element this Fermi sign is the same for the ket and for the bra and cancels. Accordingly the $n-2$ creation and annihilation operators in the ket and bra which are paired with their own Hermitean conjugate can be simply ignored. It follows, that it is sufficient to compute the diagonal matrix element of H_1 between products of only two Fermion operators. Using (2) one finds

$$\begin{aligned}\langle 0|c_{\nu_2}c_{\nu_1}\ H_1\ c^\dagger_{\nu_1}c^\dagger_{\nu_2}|0\rangle &= \frac{1}{2}\left[V(\nu_1,\nu_2,\nu_2,\nu_1)+V(\nu_2,\nu_1,\nu_1,\nu_2)\right.\\ &\qquad \left.-V(\nu_1,\nu_2,\nu_1,\nu_2)-V(\nu_2,\nu_1,\nu_2,\nu_1)\right]\\ &= V(\nu_1,\nu_2,\nu_2,\nu_1)-V(\nu_1,\nu_2,\nu_1,\nu_2).\end{aligned}$$

Here the identity $V(\nu_1,\nu_2,\nu_3,\nu_4) = V(\nu_2,\nu_1,\nu_4,\nu_3)$, which follows from exchanging the integration variables $x \leftrightarrow x'$ in (2), has been used. The second term in the last line is called the

exchange integral and is different from zero only if $\sigma_1 = \sigma_2$. From (9) we have

$$\begin{aligned} V(\nu_1,\nu_2,\nu_2,\nu_1) &= \sum_{k=0}^{\infty} c^k(l_1m_1;l_1,m_1)\; c^k(l_2m_2;l_2,m_2)\; R^k(n_1l_1,n_2l_2,n_2l_2,n_1l_1), \\ V(\nu_1,\nu_2,\nu_1,\nu_2) &= \delta_{\sigma_1\sigma_2} \sum_{k=0}^{\infty} c^k(l_1m_1;l_2,m_2)\; c^k(l_1m_1;l_2,m_2)\; R^k(n_1l_1,n_2l_2,n_1l_1,n_2l_2). \end{aligned}$$

It is customary to introduce the following abbreviations

$$\begin{aligned} a^k(lm;l'm') &= c^k(lm;lm)\;\; c^k(l'm';l'm') \\ b^k(lm;l'm') &= c^k(lm;l'm')\; c^k(lm;l'm') \\ F^k(nl;n'l') &= R^k(nl,n'l',n'l',nl) \\ G^k(nl;n'l') &= R^k(nl,n'l',nl,n'l') \end{aligned}$$

The F^k and G^k are called Slater-Condon parameters. It can be easily verified using (7) that F^k is a Coulomb-integral whereas G^k is an exchange integral. For the case of a partly filled d-shell all n_i and l_i are equal so for each k there is only one F^k and one G^k and, in fact, $G^k = F^k$. The a^k and b^k are listed for example in Appendix 20a of Slater's textbook [3] or in Appendix B of the lecture notes [6].

Finally, since ν_1 and ν_2 can be any two out of the n Fermion operators in the ket, the total diagonal matrix element of H_1 is obtained by summing over all $\frac{n(n-1)}{2}$ pairs:

$$\langle\nu|H_1|\nu\rangle = \sum_{i<j} \sum_{k=0}^{\infty} \left(a^k(l_im_i;l_jm_j)\; F^k - \delta_{\sigma_i\sigma_j}\; b^k(l_im_i;l_jm_j)\; G^k \right) \tag{11}$$

As will be seen in the next paragraph, this formula is sufficient for the analytical calculation of multiplet energies.

2.5 Analytical calculation of multiplet energies by diagonal sum-rule

The exact diagonalization procedure outlined above can be used to obtain all eigenenergies and the corresponding eigenstates of the Coulomb problem. It is a flexible numerical method of solution into which crystalline electric field, hybridization with ligand orbitals, spin-orbit coupling, and Coulomb interaction with holes in core shells, which is important for the discussion of X-ray absorption spectra, can be incorporated easily. On the other hand, multiplet theory was invented during the 1920's to explain the spectra of free atoms or ions, and at that time computers were not available. It turns out, however, that despite the apparent complexity of the problem the energies of the multiplets can be obtained analytically and this will be explained in the following.

The first ingredient is the so-called diagonal sum-rule. This is simply the well-known theorem that the sum of the eigenvalues of a Hermitean matrix H is equal to its trace $tr(H) = \sum_i H_{ii}$. This follows immediately by noting that the trace of a matrix is invariant under basis transformations, i.e., $tr(H) = tr(UHU^{-1})$ for any unitary matrix U. By choosing U to be the matrix which transforms to the basis of eigenvectors of H the diagonal sum-rule follows.

Next, one uses the fact that the Hamilton matrix is block-diagonal, with blocks defined by their values of L^z and S^z. The diagonal sum-rule then can be applied for each of the blocks separately. In addition, the dimension of these blocks decreases as L^z and S^z approach their maximum values so that the number of multiplets contained in a given block decreases.
As an example for the procedure let us consider a p^2 configuration (by particle-hole symmetry this is equivalent to a p^4 configuration). We write the Fermion operators in the form $c_{l,m,\sigma}$, i.e., we suppress the principal quantum number n. Since we have 6 possible states for a single p-electron – three m-values with two spin directions per m-value – we have 15 states for two electrons. The triangular condition implicit in the Gaunt coefficients now restricts the multipole order k to be ≤ 2. Again, only even k contribute, so that we have two Slater-Condon parameters, F^0 and F^2. The following Table which is taken from Slater's textbook [3] gives the values of the coefficients $a^k(1,m;1,m')$ and $b^k(1,m;1,m')$: We first consider the sector with $S^z = 1$.

m	m'	a^0	$25a^2$	b^0	$25b^2$
±1	±1	1	1	1	1
±1	0	1	-2	0	3
0	0	1	4	1	4
±1	∓1	1	1	0	6

Table 2: *The coefficients a^k and b^k for two p-electrons.*

The highest possible L^z is $L^z = 1$ which is obtained for a single state, $|1\rangle = c^\dagger_{1,0,\uparrow} c^\dagger_{1,1,\uparrow}|0\rangle$. We can conclude that one of the multiplets is ${}^3P$ and its energy is equal to the diagonal matrix element of $|1\rangle$ which by (11) is

$$E({}^3P) = \sum_{k\in\{0,2\}} \left(a^k(1,1;1,0) - b^k(1,1;1,0)\right) F^k = F^0 - \frac{5}{25}F^2.$$

We proceed to the sector $S^z = 0$. Here the highest possible L^z is $L^z = 2$ again obtained for only single state namely $c^\dagger_{1,1,\downarrow} c^\dagger_{1,1,\uparrow}|0\rangle$. We conclude that we also have ${}^1D$ with energy

$$E({}^1D) = \sum_{k\in\{0,2\}} a^k(1,1;1,1)\, F^k = F^0 + \frac{1}{25}F^2.$$

The two multiplets that we found so far, ${}^1D$ and ${}^3P$, comprise $5 + 9 = 14$ states - we thus have just one state missing, which can only be ${}^1S$. To find its energy, we need to consider the sector $S^z = 0$ and $L^z = 0$. There are three states in this sector: $c^\dagger_{1,0,\downarrow} c^\dagger_{1,0,\uparrow}|0\rangle$, $c^\dagger_{1,-1,\uparrow} c^\dagger_{1,1,\downarrow}|0\rangle$ and $c^\dagger_{1,-1,\downarrow} c^\dagger_{1,1,\uparrow}|0\rangle$. Two out of the three eigenvalues of the 3×3 Hamiltonian in the basis spanned by these states must be $E({}^3P)$ and $E({}^1D)$, because these multiplets also have members with $S^z = 0$ and $L^z = 0$. To obtain $E({}^1S)$ we accordingly compute the sum of the diagonal elements of the 3×3 matrix and set

$$\begin{aligned} E({}^3P) + E({}^1D) + E({}^1S) &= \sum_{k\in\{0,2\}} \left(a^k(1,0;1,0) + 2\, a^k(1,-1;1,1)\right) F^k \\ \rightarrow\ E({}^1S) &= F^0 + \frac{10}{25}F^2. \end{aligned}$$

This example shows the way of approach for multiplet calculations using the diagonal sum-rule: one starts out with a state with maximum L^z or S^z for which there is usually only a single basis state. This basis state belongs to some multiplet whose energy simply equals the 'diagonal element' of the 1×1 Hamiltonmatrix. Then one proceeds to lower S^z and/or L^z and obtains energies of additional multiplets by calculating the trace of the respective block of the Hamilton matrix and using the known energies of multiplets with higher L^z or S^z. It turns out that in this way the energies of *all* multiplets involving s, p, d, or f electrons can be expressed in terms of the Slater-Condon parameters by analytical formulas. A rather complete list can be found for example in the Appendices 21a and 21b of the textbook by Slater [3].

One point which may be helpful when reading the literature is the following: for the special case of a partly filled d-shell many authors use the so-called Racah parameters A, B and C instead of the 3 Slater-Condon parameters F^0, F^2 and F^4. The rule for conversion is simple:

$$A = F^0 - \frac{49}{441}F^4 \qquad B = \frac{1}{49}F^2 - \frac{5}{441}F^4 \qquad C = \frac{35}{441}F^4.$$

The Racah-parameters have been introduced because the analytical formulas for the energies of the multiplets of d^n as derived by the diagonal sum-rule look nicer when they are expressed in terms of them. For example Griffith [4] gives multiplet energies in terms of the Racah-parameters in his Table 4.6.

As stated above, multiplet theory was originally developed to discuss the spectra of atoms or ions in the gas phase. The question then arises, as to what are the values of the Slater-Condon parameters. Of course one might attempt to compute these parameters using, e.g., Hartree-Fock wave functions in the expression (7). It turns out, however, that very frequently the number of multiplets considerably exceeds the number of relevant Slater-Condon parameters. In the case of the p^2 configuration we had three multiplets, ^3P, ^1D and ^1S, but only two Slater-Condon parameters F^0 and F^2. This would suggest to obtain the values of the Slater-Condon parameters by fit to the spectroscopic data and the textbook by Slater [3] contains a vast amount of data which are analyzed in this way. For the p^2 configuration we restrict ourselves to a simple cross check. Using the above formulae and eliminating the F's we find:

$$r = \frac{E(^1S) - E(^1D)}{E(^1D) - E(^3P)} = \frac{3}{2}. \tag{12}$$

This relation should be obeyed by all ions with two p-electrons outside filled shells, e.g., the series C, N^{1+} and O^{2+} or two holes in a filled p-shell such as the series O and F^+. The energies of these multiplets have been measured with high precision and are available in databases [7] and Table 3 shows the resulting values of r. For the first row elements the deviation is about 25%, for the second row only about 5%. We recall that multiplet theory in its simplest form corresponds to first order degenerate perturbation theory, where H_0 contains the orbital energies and H_1 the Coulomb interaction between electrons in one shell. It therefore ignores various scattering processes which may lead to inaccuracies.

p^2	C	N^+	O^{2+}	Si	P^+	S^{2+}
	1.124	1.134	1.130	1.444	1.430	1.399
p^4	O	F^+	S	Cl^+		
	1.130	1.152	1.401	1.392		

Table 3: *The ratio (12) for various Atoms and Ions with p^2 and p^4 configurations ouside a closed shell.*

2.6 Spin-orbit coupling

As the last problem in this section on free atoms or ions we briefly discuss spin-orbit coupling. The corresponding Hamiltonian is

$$H_{SO} = \lambda_{SO} \sum_{i=1}^{n} \boldsymbol{L}_i \cdot \boldsymbol{S}_i = \lambda_{SO} \sum_{i=1}^{n} \left(L_i^z S_i^z + \frac{1}{2}(L_i^+ S_i^- + L_i^- S_i^+) \right).$$

where $\boldsymbol{L}_i$ ($\boldsymbol{S}_i$) are the operator of orbital (spin) angular momentum of the i^{th} electron. The first term on the right hand side can be translated into second quantized form easily:

$$H_{SO}^{\parallel} = \frac{\lambda_{SO}}{2} \sum_{m=-l}^{l} m \, (c_{l,m,\uparrow}^{\dagger} c_{l,m,\uparrow} - c_{l,m,\downarrow}^{\dagger} c_{l,m,\downarrow}). \tag{13}$$

As regards the transverse part, we note [5] that the only nonvanishing matrix elements of the orbital angular momentum raising/lowering operator are $\langle l, m \pm 1 | l^{\pm} | l, m \rangle = \sqrt{(l \mp m)(l \pm m + 1)}$ whence

$$H_{SO}^{\perp} = \frac{\lambda_{SO}}{2} \sum_{m=-l}^{l-1} \sqrt{(l-m)(l+m+1)} \, (c_{l,m+1,\downarrow}^{\dagger} c_{l,m,\uparrow} + c_{l,m,\uparrow}^{\dagger} c_{l,m+1,\downarrow}). \tag{14}$$

It is easy to see that H_{SO} changes sign under the particle-hole transformation (10). This means that, e.g., the multiplets of d^n and d^{10-n} have the same Coulomb energies, but the splitting due to spin-orbit coupling is opposite. Since the value of λ_{SO} is positive [5], this means that for less than half-filled shells the ground state has the minimum value of J possible, whereas for more than half-filled shells the ground state has the maximum possible value of J, i.e., Hund's third rule.

Spin-orbit coupling can be implemented rather easily into the numerical procedure, the main difficulty again is keeping track of the Fermi sign. Due to the fact that neither L^z nor S^z are conserved anymore the corresponding reduction of the Hilbert space is no longer possible. In transition metal compounds the spin-orbit coupling constant λ_{SO} for the $3d$ shell is rather small, of order $\lambda_{SO} \approx 0.05$ eV. Still, if the ground state of a given ion has a nonvanishing spin, spin orbit coupling will determine how this spin orients itself in an ordered phase, i.e., *magnetic anisotropy*. In the rare earth elements spin-orbit coupling in the $4f$ shell is of comparable magnitude as the Coulomb repulsion. There, taking spin-orbit coupling into account is mandatory.

3 Effects of the environment in the crystal

So far we have considered a single ion in vacuum. Clearly, one might ask if the results obtained in this limit retain any relevance once the ion is embedded into a solid and this will be discussed in the following. It will become apparent that the small spatial extent of the $3d$ radial wave function $R_{3,2}(r)$ strongly suppresses any effect of the environment in a solid, so that in many cases the main effect of embedding the ion into a solid is the partial splitting of the multiplets of the free ion.

In many transition metal compounds the $3d$ ions are surrounded by an approximately octahedral or tetrahedral 'cage' of nonmetal ions such as Oxygen, Sulphur, Arsenic. An example for octahedral coordination is provided by the perovskite structure. These nearest neighbor ions, which will be called 'ligands' in the following, have a twofold effect: first, they produce a static electric field – the so-called *crystalline electric field* or CEF – and second there may be *charge transfer* that means electrons from a filled ligand orbital may tunnel into a $3d$-orbital of the transition metal ion due to the overlap of the respective wave functions.

3.1 Crystalline electric field

Let us first consider the crystalline electric field, whereby we model the ligands simply by n_c point charges $Z_i e$ at the positions $\boldsymbol{R}_i$. We denote the electrostatic potential due to these point charges by $V_{\mathrm{CEF}}(\boldsymbol{r})$ and find for the respective Hamiltonian [2]

$$\begin{aligned} H_{\mathrm{CEF}} &= \sum_{i,j} V_{\mathrm{CEF}}(\nu_i,\nu_j)\; c^\dagger_{\nu_i} c_{\nu_j}, \\ V_{\mathrm{CEF}}(\nu_1,\nu_2) &= \int dx\; \psi^*_{\nu_1}(x)\; V_{\mathrm{CEF}}(\boldsymbol{r})\; \psi_{\nu_2}(x). \end{aligned} \tag{15}$$

The radial dependence of the $3d$ wave functions $\psi_\nu(x)$ is given by $R_{3,2}(r)$ which differs appreciably from zero only in a narrow range $r \leq r_{3d}$. Assuming that $r_{3d} < R_i$ for all i we obtain $V_{\mathrm{CEF}}(\boldsymbol{r})$ from the multipole expansion (4)

$$\begin{aligned} V_{\mathrm{CEF}}(\boldsymbol{r}) &= -\frac{Z_{av}e^2}{R_{av}} \sum_{k=0}^{\infty} \sum_{m=-k}^{k} \gamma_{k,m} \left(\frac{r}{R_{av}}\right)^k \sqrt{\frac{4\pi}{2k+1}}\, Y_{k,m}(\Theta,\phi), \\ \gamma_{k,m} &= \sqrt{\frac{4\pi}{2k+1}} \sum_{i=1}^{n_c} \frac{Z_i}{Z_{av}} \left(\frac{R_{av}}{R_i}\right)^{k+1} Y^*_{k,m}(\Theta_i,\phi_i). \end{aligned} \tag{16}$$

Here we have introduced the avergage distance and charge of the ligands, R_{av} and Z_{av}. In calculating the matrix elements $V_{\mathrm{CEF}}(\nu_1,\nu_2)$ the integral over the polar angles (Θ,ϕ) again gives a Gaunt coefficient. For a d-shell it again follows from the triangular condition that $k \leq 4$ and from parity that k be even. The term with $k = 0$ gives only a constant shift and can be

omitted so that

$$\begin{aligned} V_{\mathrm{CEF}}(\nu_1,\nu_2) &= \sum_{k\in\{2,4\}} \gamma_{k,m_1-m_2}\; c^k(2,m_1;2,m_2)\; I_k, \\ I_k &= -\frac{Z_{av}e^2}{R_{av}}\;\left(\frac{r_{3d}}{R_{av}}\right)^k \int_0^\infty d\rho\;\rho^{k+2}\;\tilde{R}^2_{nl}(\rho), \end{aligned}$$

with the rescaled and normalized radial wave function $\tilde{R}_{nl}(\rho) = r_{3d}^{3/2} R_{nl}(\rho r_{3d})$. Note that I_k has the correct dimension of energy and that the integral is dimensionless and of order unity. For $r_{3d}/R_{av} \ll 1$, which we expect to hold due to the small extent of the $3d$ radial wave function, the sum can be terminated after the lowest $k > 0$ for which there is a nonvanishing contribution, i.e., where $\gamma_{k,m}$ does not vanish. As was the case for the Coulomb interaction, the CEF can be described by very few – in fact only one if only the lowest order in r_{3d}/R_{av} is kept – parameters which depend on the radial wave function $R_{3,2}(r)$. These parameters again are frequently fitted to experiment.

The actual form of the matrix elements depends on the geometry of the cage of ligands via the sum in $\gamma_{k,m}$. For the frequently considered case of an ideal octahedron of identical charges where $R_i = R = R_{av}$ and $Z_i = Z = Z_{av}$ one finds $\gamma_{k,m} = 0$ for $0 < k < 4$ and

$$\begin{aligned} \gamma_{4,4} &= \sqrt{\frac{35}{8}} \\ \gamma_{4,0} &= \sqrt{\frac{49}{4}} \end{aligned} \tag{17}$$

as well as $\gamma_{4,-4} = \gamma_{4,4}$. Using the tabulated values of the $c^4(2,m;2,m')$ (see Appendix), $V_{\mathrm{CEF}}(\nu_1,\nu_2)$ can be written down as a matrix in the indices m_1 and m_2:

$$V_{\mathrm{CEF}}(\nu_1,\nu_2) = \frac{I_4}{6}\begin{pmatrix} 1 & 0 & 0 & 0 & 5 \\ 0 & -4 & 0 & 0 & 0 \\ 0 & 0 & 6 & 0 & 0 \\ 0 & 0 & 0 & -4 & 0 \\ 5 & 0 & 0 & 0 & 1 \end{pmatrix}. \tag{18}$$

This matrix has the eigenvalues I_4 (twofold degenerate) and $-2I_4/3$ (threefold degenerate). If the ligands are O^{2-} ions, $Z = -2$ and $I_4 > 0$. For historical reasons the splitting between the eigenvalues is frequently called $10Dq$ so that in our point charge model $Dq = I_4/6$. The two eigenfunctions belonging to the eigenvalue $6Dq$ are the real valued e_g-type spherical harmonics, the three eigenvalues belonging to the eigenvalue $-4Dq$ are the real valued t_{2g}-type spherical harmonics, see the lecture by E. Pavarini. Lastly, we note that H_{CEF} changes sign under the particle-hole transformation (10). In a solid the multiplets of d^n and d^{10-n} thus are split in opposite ways.

The implementation of the CEF in an exact diagonalization program is rather obvious. As an example Fig. 3 shows the eigenenergies of the d^8 and d^7 configuration with Coulomb interaction and octahedral CEF as $10Dq$ is increasing. Such plots of crystal field levels versus $10Dq$ are

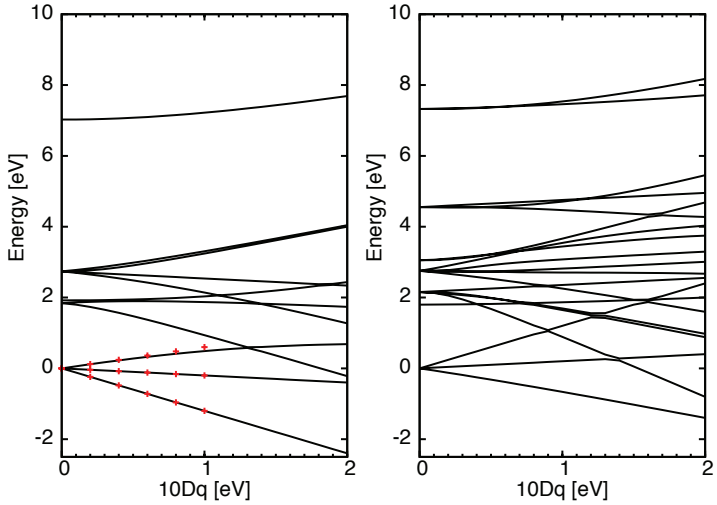

Fig. 3: *Examples for Tanabe-Sugano diagrams: the splitting of multiplets of d^8 (left) and d^7 (right) for increasing $10Dq$. The Slater-Condon parameters have the values given in Table 2. The symbols in the diagram for d^8 give the energies calculated analytically by use of the Wigner-Eckart theorem.*

called Tanabe-Sugano diagrams after the authors who first derived them [8]. One realizes that the highly degenerate multiplets of the free ion are split into several levels of lower degeneracy by the CEF, which is to be expected for a perturbation which lowers the symmetry. Note that the components into which a given multiplets splits up all have the same spin as the multiplet itself. This is because the spin of an electron does not 'feel' an electrostatic potential – or, more precisely, because the operator of total spin commutes with any operator which acts only on the real-space coordinates $\boldsymbol{r}_i$ of the electrons. Only the introduction of spin-orbit coupling, as discussed in the preceding section, leads to a coupling between spin and environment of a given ion and thus may lead to magnetic anisotropy.

3.2 Analytical results by application of the Wigner-Eckart theorem

In addition to the purely numerical approach, many results can be obtained by invoking the Wigner-Eckart theorem. To formulate this theorem we first need to define a tensor operator. Let $\boldsymbol{J}$ be some angular momentum operator with eigenfunctions $|j,m\rangle$. This means that the three components of $\boldsymbol{J}$ have to obey the commutation relations $[J_\alpha, J_\beta] = i\epsilon_{\alpha\beta\gamma}J_\gamma$. It follows [5] that the kets $|j,m\rangle$ obey $\boldsymbol{J}^2|j,m\rangle = j(j+1)|j,m\rangle$, $J^z|j,m\rangle = m|j,m\rangle$ and $J^\pm|j,m\rangle = \sqrt{(j\mp m)(j\pm m+1)}|j,m\pm 1\rangle$.
A rank-j tensor operator then is a set of $2j+1$ operators $O_{j,m}$ which obey $[J^z, O_{j,m}] = mO_{j,m}$ and $[J^\pm, O_{j,m}] = \sqrt{(j\mp m)(j\pm m+1)}O_{j,m\pm 1}$. This means that these operators transform amongst themselves like eigenfunctions of angular momentum. Note that a tensor operator always needs to refer to some angular momentum operator. As an example we choose $\boldsymbol{J}$ to be the orbital angular momentum of a single particle. Then, the set of $2l+1$ spherical harmonics $Y_{l,m}(\Theta,\phi)$ forms a rank-l tensor operator. Namely by acting with a component of $\boldsymbol{J}$ onto

the product $Y_{l,m}(\Theta,\phi)|\Psi(r,\Theta,\phi)\rangle$ with an arbitrary wave function Ψ, the differential operators included in $\boldsymbol{J}$ will always produce two terms $JY_{l,m}|\Psi\rangle = (JY_{l,m})|\Psi\rangle + Y_{l,m}J|\Psi\rangle$ so that $[J,Y_{l,m}]|\Psi\rangle = (JY_{l,m})|\Psi\rangle$ and since $|\Psi\rangle$ is arbitrary the tensor operator property of $Y_{l,m}$ follows. In exactly the same way, if $\boldsymbol{J}$ is the total angular momentum of n electrons the $2l+1$ functions $\sum_{i=1}^{n} Y_{l,m}(\Theta_i,\phi_i)$ form a rank-l tensor operator as well. For a $3d$ shell with n electrons the operator describing the CEF is $H_{\mathrm{CEF}} = \sum_{i=1}^{n} V_{\mathrm{CEF}}(\boldsymbol{r}_i)$ with $V_{\mathrm{CEF}}(\boldsymbol{r})$ given by (16). H_{CEF} therefore is a sum of components of a tensor operator and this property makes the Wigner-Eckart theorem useful in the present case.

The theorem itself states that the matrix elements of *any two* rank-j tensor operators between eigenstates of their respective angular momentum operator are proportional to one another, whereby the constant of proportionality is *independent of the values of* m

$$\langle\alpha,j',m'|O_{J,M}|\alpha,j,m\rangle = C(\alpha,\beta,j',j,J)\langle\beta,j',m'|\bar{O}_{J,M}|\beta,j,m\rangle.$$

The symbols α and β stand for some unspecified 'additional' quantum numbers. Note that neither m', nor M, nor m appear in the constant of proportionality C. The deeper reason for this theorem is that the dependence of the matrix elements on m', M and m is given solely by Clebsch-Gordan coefficients. More precisely, an alternative way of stating the theorem [5] is that

$$\langle\alpha,j',m'|O_{J,M}|\alpha,j,m\rangle = A(\alpha,j,j',J)\langle j'm'Jj|JMjm\rangle$$

where $\langle j'm'Jj|JMjm\rangle$ is a Clebsch-Gordan coefficient. The above version then follows with $C(\alpha,\beta,j,j',J) = A(\beta,j,j',J)/A(\alpha,j,j',J)$. The quantity $A(\alpha,j,j',J)$ is known as the reduced matrix element.

To illustrate the application of the theorem we now use it to calculate the splitting of the ${}^3F$ ground state multiplet of d^8, which is equivalent to d^2, in ideal octahedral coordination. On the left hand side we accordingly choose $|\alpha,j,m\rangle = |{}^3F,m\rangle$ where $|{}^3F,m\rangle$ is the member of the ${}^3F$ multiplet with $L^z = m$ and $S^z = 1$ (the value of S^z is arbitrary and the final results of course must not depend on this choice). The $|{}^3F,m\rangle$ are eigenfunctions of the total orbital momentum operator. For O_{JM} we choose $\sum_{i=1}^{n} V_{\mathrm{CEF}}(\boldsymbol{r}_i)$, where $V_{\mathrm{CEF}}(\boldsymbol{r})$ is the CEF potential (16) and the sum is over all n electrons. For ideal octahedral coordination this is a linear combination of components of a tensor operator of rank 4, see (16) and (17).

On the right hand side we choose $|\beta,j,m\rangle = Y_{3,m}(\Theta,\phi)$ and for the tensor operator $\bar{O}_{J,M}$ the expression

$$\tilde{V}_{\mathrm{CEF}}(\Theta,\phi) = \sum_{m=-4}^{4} \gamma_{4,m} Y_{4,m}(\Theta,\phi),$$

i.e., the dimensionless version of the CEF potential (16) but now *for a single particle*. The Wigner-Eckart theorem then tells us that the secular determinant of the CEF potential between the $|{}^3F,m\rangle$ is, up to a constant factor C, the same as the matrix $\langle Y_{3,m'}|\tilde{V}_{\mathrm{CEF}}|Y_{3,m}\rangle$. Above we found that the matrix elements of $\tilde{V}_{\mathrm{CEF}}$ are $\gamma_{4,m'-m}\ c^4(3,m';3,m)$ and using the tabulated

$c^4(3m;3m')$ (see Appendix) this becomes

$$\tilde{V}_{\rm CEF} \;=\; \frac{7}{66}\begin{pmatrix} 3 & 0 & 0 & 0 & \sqrt{15} & 0 & 0 \\ 0 & -7 & 0 & 0 & 0 & 5 & 0 \\ 0 & 0 & 1 & 0 & 0 & 0 & \sqrt{15} \\ 0 & 0 & 0 & 6 & 0 & 0 & 0 \\ \sqrt{15} & 0 & 0 & 0 & 1 & 0 & 0 \\ 0 & 5 & 0 & 0 & 0 & -7 & 0 \\ 0 & 0 & \sqrt{15} & 0 & 0 & 0 & 3 \end{pmatrix}. \tag{19}$$

Since we are not interested in constant factors we drop the factor of $7/66$. The matrix on the right hand side then can be decomposed into 2×2 blocks and we obtain the eigenvalues -12 (once), -2 (three times) and $+6$ (three times). The Wigner-Eckart theorem now tells us that the ${}^3F$ ground state multiplet of both d^2 and of d^8 splits up in the same way, namely into three levels, with degeneracies $1, 3$ and 3 and energies $-12C$, $-2C$ and $6C$.
To 'gauge' the calculation and determine the constant C we now need to evaluate the CEF energy of *one* particular state of the true ${}^3F$ multiplet. To that end we note that the CEF eigenstates originating from the ${}^3F$ multiplet are expressed in terms of the $|{}^3F,m\rangle$ in *exactly the same way* as the eigenstates of the matrix (19). By inspection of the matrix (19) we see, however, that the eigenvalue $+6$ has one particularly simple eigenvector, namely $(0,0,0,1,0,0,0)$. This corresponds to the state $|{}^3F,m=0\rangle$. This special state now can be calculated as follows: by starting with the member of ${}^3F$ with maximum m, namely $|{}^3F,3\rangle = c^\dagger_{2,1,\uparrow}c^\dagger_{2,2,\uparrow}|0\rangle$, acting repeatedly with L^- and normalizing we can work ourselves down to $m=0$:

$$\begin{aligned}
|{}^3F,3\rangle &= c^\dagger_{2,1,\uparrow}c^\dagger_{2,2,\uparrow}|0\rangle,\\
|{}^3F,2\rangle &= c^\dagger_{2,0,\uparrow}c^\dagger_{2,2,\uparrow}|0\rangle,\\
|{}^3F,1\rangle &= \left(\sqrt{\frac{2}{5}}\,c^\dagger_{2,0,\uparrow}c^\dagger_{2,1,\uparrow} + \sqrt{\frac{3}{5}}\,c^\dagger_{2,-1,\uparrow}c^\dagger_{2,2,\uparrow}\right)|0\rangle,\\
|{}^3F,0\rangle &= \left(\sqrt{\frac{4}{5}}\,c^\dagger_{2,-1,\uparrow}c^\dagger_{2,1,\uparrow} + \sqrt{\frac{1}{5}}\,c^\dagger_{2,-2,\uparrow}c^\dagger_{2,2,\uparrow}\right)|0\rangle.
\end{aligned}$$

From the Wigner-Eckart theorem we now know that the last state, $|{}^3F,0\rangle$, is an eigenstate of the Coulomb energy plus CEF. Accordingly, its CEF-energy is simply the expectation value $\langle{}^3F,0|H_{\rm CEF}|{}^3F,0\rangle$ with $H_{\rm CEF}$ given by (15) with (18). This is easily calculated and we obtain the constant C as:

$$6C = \frac{I_4}{6}\left(\frac{4}{5}\,(-8) + \frac{1}{5}\,2\right) = -I_4,$$

so that $C=-I_4/6=-Dq$. We thus find that in octahedral coordination ${}^3F$ of d^2 splits into three levels with $E=-6Dq$ (3-fold degenerate), $E=2Dq$ (3-fold) and $E=12Dq$ (1-fold). For d^8 particle-hole symmetry tells us that the sign of the CEF splitting has to be inverted whence we find the energies and degeneracies $E=-12Dq$ (1-fold), $E=-2Dq$ (3-fold) and $E=6Dq$ (3-fold). This splitting of the lowest multiplet can be nicely seen in Fig. 3. In the

result obtained by exact diagonalization the upper level with $E = 6Dq$ 'bends downward' for larger $10Dq$. The reason is that the CEF mixes the ${}^3F$ and ${}^3P$ multiplets and the resulting level repulsion for large $10Dq$ leads to the deviation from the linear behaviour, which gives only the asymptotic behaviour for $10Dq \to 0$. Note the tremendous simplification which occurs in this way, because the $|{}^3F, m\rangle$ actually are linear combinations of Slater-determinants (1) with coefficients which have to be obtained from diagonalizing the full Coulomb-Hamiltonian! Historically, by using the Wigner-Eckart theorem together with skilfull application of group theory, the energies and wave functions of transition metal ions in various coordinations in fact were calculated analytically and without the use of a computer. This is how the Tanabe-Sugano diagrams were obtained originally.

3.3 Charge transfer

We proceed to a discussion of charge transfer. This means that electrons can tunnel from ligand orbitals into $3d$ orbitals, so that the number of electrons in the d-shell fluctuates. To deal with this we need to enlarge our set of Fermion operators $c^\dagger_\nu / c_\nu$ by operators $l^\dagger_\mu / l_\mu$ which create/annihilate electrons in orbitals centered on ligands. The compound index μ for the ligand operators also must include the index i of the ligand: $\mu = (i, n, l, m, \sigma)$. The Hamiltonian then would read

$$H = \sum_{i,j} \left(t_{\nu_i,\mu_j}\ c^\dagger_{\nu_i} l_{\mu_j} + H.c. \right) + \sum_j \epsilon_{\mu_j} l^\dagger_{\mu_j} l_{\mu_j} + \sum_i \epsilon_{\nu_i} c^\dagger_{\nu_i} c_{\nu_i}. \tag{20}$$

The *hybridization integrals* t_{ν_i,μ_j} may be expressed in terms of relatively few parameters by using the famous *Slater-Koster tables*, see the lecture by E. Pavarini. For example, if only the p-orbitals of the ligands are taken into account, which applies to oxides of transition metals such as perovskites, there are just two relevant parameters, $V_{pd\sigma}$ and $V_{pd\pi}$. Estimates for these may be obtained from fits to LDA band structures. If electrons are allowed to tunnel between d-shell and ligand orbitals the site energies ϵ_{μ_j} become relevant as well. Estimating the d-shell site energies from LDA calculations is tricky due to the *double counting problem*: the energies of the d-orbitals extracted from band structure calculations involve the Hartree-potential, which is also included in the diagonal matrix elements of the multiplet Hamiltonian and thus must be subtracted in some way. Recently, considerable interest has emerged in the determination of such parameters.

The use of the Slater-Koster tables brings about a slight complication in that these are formulated in terms of the real-valued spherical harmonics $Y_\alpha(\Theta, \phi)$ which are linear combinations of the original $Y_{2,m}(\Theta, \phi)$. However, these sets of functions are related by a simple unitary transformation. We again specialize to the case where the ligands are oxygen ions which form an ideal octahedron with the transition metal ion in the center of gravity of the octahedron. In this case the number of relevant ligand orbitals can be reduced considerably. Namely, for each of the real-valued transition metal $3d$ orbitals $Y_\alpha(\Theta, \phi)$ there is precisely one linear combination of O $2p$ orbitals on the ligands, L_α, which hybridizes with them. The Hamiltonian then simplifies

to

$$H_{\rm hyb} = 2\,V_{pd\pi}\,\sum_{\alpha\in t_{2g}}\sum_{\sigma}\left(c^{\dagger}_{\alpha,\sigma}l_{\alpha\sigma}+H.c.\right)+\sqrt{3}\,V_{pd\sigma}\,\sum_{\alpha\in e_g}\sum_{\sigma}\left(c^{\dagger}_{\alpha,\sigma}l_{\alpha\sigma}+H.c.\right).$$

By inserting the unitary transformation $c^{\dagger}_{\alpha}=\sum_{m=-2}^{2}\,U_{\alpha,m}c^{\dagger}_{m,\sigma}$ to transform to the original complex spherical harmonics this is easily included into the formalism. In the exact diagonalization program this means that the number of orbitals has to be doubled, because we have the five combinations L_α, each of which can accomodate an electron of either spin direction. This leads to a quite drastic increase in the dimension of the Hilbert space but using, e.g., the Lanczos algorithm, see the lecture by E. Koch [9], the problem still is tractable. $H_{\rm hyb}$ then simply transfers electrons from ligand orbitals to d-orbitals and vice versa and is easy to implement.

4 Cluster calculation of photoemission and X-ray absorption spectra

In the preceding section we have discussed the general formalism for exact diagonalization of a cluster consisting of a transition metal ion and its nearest neighbor ions ('ligands'). Thereby the following terms were included into the Hamiltonian: the Coulomb repulsion between the electrons in the $3d$ shell, the electrostatic field produced by the ligands, charge transfer between the ligands and the transition metal d orbitals and, possibly, the spin orbit coupling in the $3d$ shell. By diagonalizing the resulting Hamilton matrix we can obtain the eigenfunctions $|\Psi_\nu\rangle$ and their energies E_ν and these can be used to simulate various experiments on transition metal compounds such as electron spectroscopy, optical spectroscopy, electron spin resonance or inelastic neutron scattering. It has turned out that these simulations are in fact spectacularly successful. In many cases calculated spectra can be overlayed with experimental ones and agree peak by peak. Nowadays complete packages for such cluster simulations are available, and these are used routinely for the interpretation of, e.g., electron spectroscopy [10]. This shows in particular that the multiplets of the free ion – suitably modified by the effects of crystalline electric field and charge transfer – persist in the solid and thus are essential for a correct description of transition metal compounds. In the following, we want to explain this in more detail and consider photoelectron spectroscopy. In this lecture only a very cursory introduction can be given, there are however several excellent reviews on the application of multiplet theory to the simulation of photoelectron spectroscopy [11–13].

In a valence-band photoemission experiment electromagnetic radiation impinges on the sample which then emits electrons – this is nothing but the well-known photo-electric effect. 'Valence band photoemission' means that the photoelectrons are ejected from states near the Fermi level so that, to simplest approximation, an ion in the solid undergoes the transition $d^n \rightarrow d^{n-1}$ (note that this ignores charge transfer, which in fact is quite essential!). What is measured is the current I of photoelectrons as a function of their kinetic energy E_{kin} and possibly the polar angles (Θ,ϕ) relative to the crystallographic axes of the sample. Frequently one measures the angle-integrated spectrum, obtained by averaging over (Θ,ϕ), or rather: measuring a polycrystalline

sample. A further parameter which strongly influences the shape of the spectrum $I(E_{kin})$ is the energy $h\nu$ of the incident photons. At sufficiently high $h\nu$ the photoionization cross-section for the transition metal $3d$-orbitals is significantly larger than for the other orbitals in the solid so that the photoelectrons in fact are emitted almost exclusively the $3d$-orbitals. This is often called XPS – for X-ray photoemission spectroscopy.

The theory of the photoemission process is complicated [14, 15] but with a number of simplifying assumptions one can show that the photocurrent $I(E_{kin})$ measured in an angle-integrated photoemission at high photon energy is proportional to the so-called single-particle spectral function

$$\begin{aligned} A(\omega) &= -\frac{1}{\pi Z}\Im \sum_{m=-2}^{2}\sum_{\mu} e^{-\beta E_\mu} \left\langle \Psi_\mu \left| c^\dagger_{3,2,m,\sigma} \frac{1}{\omega + (H - E_\mu) + i0^+} c_{3,2,m,\sigma} \right| \Psi_\mu \right\rangle \\ &= \frac{1}{Z}\sum_{m=-2}^{2}\sum_{\mu,\nu} e^{-\beta E_\mu} |\langle \Psi_\nu | c_{3,2,m,\sigma} | \Psi_\mu \rangle|^2 \delta(\omega + (E_\nu - E_\mu)). \end{aligned} \tag{21}$$

Here H is the Hamiltonian describing the solid, $|\Psi_\mu\rangle$ and E_μ denote the eigenstates of H with a fixed electron number N_e. Moreover $\beta = (k_B T)^{-1}$ where k_B is the Boltzmann constant, T the temperature, and $Z = \sum_\mu \; exp(-\beta E_\mu)$. The operator $c_{3,2,m,\sigma}$ removes an electron from a $3d$-orbital. In the thermodynamical limit the results will not depend on the position of the ion in the sample and accordingly we have suppressed the site index on $c_{3,2,m,\sigma}$. After removal of the electron the sample then remains in an eigenstate $|\Psi_\nu\rangle$ with $N_e - 1$ electrons and energy E_ν. The relation between E_{kin} and ω follows from energy conservation:

$$h\nu + E_\mu = E_{kin} + \Phi + E_\nu$$

The left and right hand sides of this equation are the energies of the system before (solid+photon) and after (solid + photo-electron) the photoemission process. Here Φ is the so-called work function, i.e., the energy needed to transverse the potential barrier at the surface of the solid (this needs to be introduced because the measured kinetic energy E_{kin} is the one *in vacuum*). It follows from the δ function in the second line of (21) that we have to put $I(E_{kin}) \propto A(E_{kin} + \Phi - h\nu)$.

We now make the approximation, introduced by Fujimori and Minami [16], and evaluate $A(\omega)$ by replacing the energies and wave functions of the solid by those of the octahedral cluster. If we moreover let $T \to 0$ the sum over μ becomes a sum over the m denerate gound states of the cluster and $e^{-\beta E_\mu}/Z \to 1/m$. The underlying assumption is that the coupling of the clusters to a solid will predominantly broaden the ionization states of the cluster to 'bands' of not too large bandwidth. This broadening is usually simulated by replacing the δ-functions by Lorentzians. To compare to a measured spectrum the calculated spectrum often is convoluted with a Gaussian to simulate the finite energy resolution of the photoelectron detector. The upper version of the equation (21) is suitable for using the Lanczos algorithm whereas the lower one is better suited if the eigenstates and energies have been obtained by full diagonalization of the eigenvalue problem.

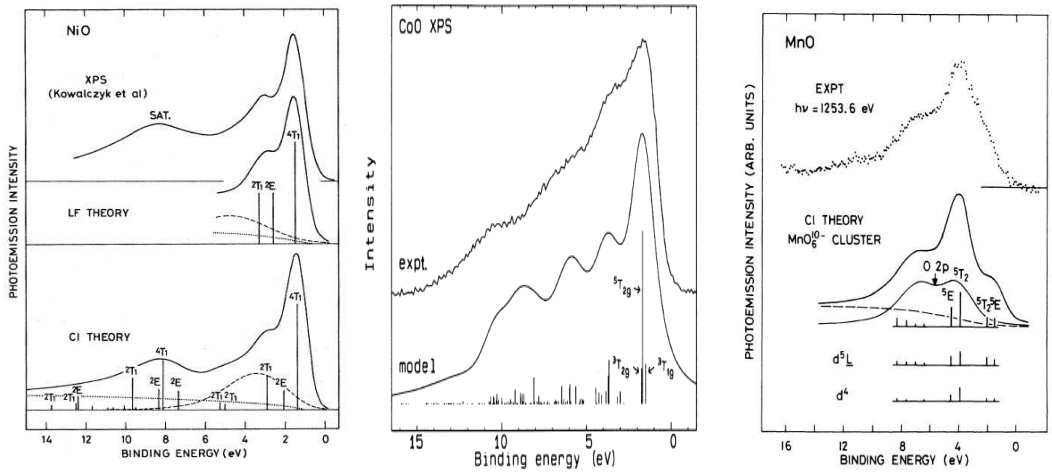

Fig. 4: *Comparison of experimental valence band photoemission spectra and results from cluster calculations: NiO (left), CoO(center), MnO(right). Reprinted with permission from [16], Copyright 1984, from [17], Copyright 1991, and from [18], Copyright 1990 by the American Physical Society.*

Fig. 4 shows various examples from the literature where measured XPS-spectra are compared to spectra calculated by the procedure outlined above. The sticks in some of the theoretical spectra mark the final state energies E_ν and are labeled by the symbols of the irreducible representation of the octahedral group, see the lecture by E. Pavarini, to which the corresponding final state wave function $|\Psi_\nu\rangle$ belongs. The figure shows that the agreement between the theoretical spectra and experiment is usually rather good. It is interesting to note that the three oxides shown in the figure all have the same crystal structure, namely the rock-salt structure. Since, moreover, Ni, Co and Mn are close neighbors in the periodic table, LDA predicts almost identical band structures, the main difference being an upward shift of the chemical potential with increasing nuclear charge of the transition metal. Despite this, the XPS spectra differ considerably and this change is reproduced very well by the theoretical spectra. This is clear evidence that the shape of the spectra is determined not so much by the single particle band structure, but by the multiplet structure of the transition metal ion, which in turn depends on its valence and spin state.

Next, we discuss X-ray absorption. In an X-ray absorption experiment an electron from either the $2p$ or the $3p$ shell absorbs an incoming X-ray photon and is promoted to the $3d$-shell via a dipole transition. In terms of electron configurations, the transition thus is $2p^6 3d^n \rightarrow 2p^5 3d^{n+1}$ (for definiteness we will always talk about the $2p$ shell from now on). Of particular interest here is the range of photon energies just above the threshold where the energy of the photon is sufficient to lift the core electron to an unoccupied state. Above this threshold the X-ray absorption coefficient $\kappa(\omega)$ rises sharply, which is called an absorption edge. The energy of the edge thereby is characteristic for a given element so that one can determine unambiguously which atom in a complex solid or molecule is probed. The ω-dependence of $\kappa(\omega)$ in an energy range of a few eV above the absorption edge – called NEXAFS for 'Near Edge X-ray Absorption Fine

Struture' – contains information about the initial state of the $3d$ shell, that means its valence and spin state, and this information can be extracted by using cluster calculations. The measured quantity in this case is

$$\begin{aligned}\kappa(\omega) &= -\frac{1}{\pi Z}\Im \sum_{m=-2}^{2}\sum_{\mu} e^{-\beta E_\mu} \left\langle \Psi_\mu \left| D(\boldsymbol{n}) \frac{1}{\omega-(H-E_\mu)+i0^+} D(\boldsymbol{n}) \right| \Psi_\mu \right\rangle \\ &= \frac{1}{Z}\sum_{m=-2}^{2}\sum_{\mu,\nu} e^{-\beta E_\mu} |\langle \Psi_\nu | D(\boldsymbol{n}) | \Psi_\mu \rangle|^2 \delta(\omega-(E_\nu-E_\mu)). \end{aligned} \tag{22}$$

This is very similar to the single-particle spectral function (21), the only difference is that now the dipole operator $D(\boldsymbol{n})$ (which will be defined later on) appears in place of the electron annihilation operator $c_{3,2,m,\sigma}$. This also implies that the number of electrons in the final states $|\Psi_\nu\rangle$ now is equal to that in the initial states $|\Psi_\mu\rangle$.

We again make the approximation to use the octahedral cluster to simulate this experiment. The initial state for this experiment – $2p^6 3d^n$ – is simply the ground state of the cluster. More difficult is the final state, $2p^5 3d^{n+1}$. This has a hole in the $2p$ shell so that the single-particle basis has to be enlarged once more to comprise also the 6 spin-orbitals available for $2p$ electrons. We may restrict the basis, however, to include only states with 5 electrons in these 6 spin-orbitals, so that the dimension of the Hilbert space increases only by a moderate factor of 6. The spin-orbit coupling constant $J_{SO,2p}$ in the $2p$ shell of $3d$ transition metals is of order 10 eV so we definitely need to include spin orbit coupling in the $2p$-shell. Here the forms (13) and (14) with $l=1$ can be used. The orbital angular momentum $l=1$ and the spin of $\frac{1}{2}$ can be coupled to a total angular momentum of either $J=\frac{3}{2}$ or $J=\frac{1}{2}$. Using the identity

$$\langle \boldsymbol{L}\cdot\boldsymbol{S}\rangle = \frac{1}{2}\left(J(J+1)-L(L+1)-S(S+1)\right)$$

we expect a splitting of $E_{\frac{3}{2}}-E_{\frac{1}{2}}=\frac{\lambda_{SO}}{2}(\frac{15}{4}-\frac{3}{4})=\frac{3\lambda_{SO}}{2}$. This means that we actually have two edges, separated by $\frac{3\lambda_{SO}}{2}\approx 10-15$ eV for $2p$ core levels. The one for lower photon energy – called the L_3 edge – is due to electrons coming from ${}^2P_{3/2}$, the one for higher photon energy (L_2-edge) due to electrons from ${}^2P_{1/2}$. Since there are 4 ${}^2P_{3/2}$ states but only 2 ${}^2P_{1/2}$ states the L_3 edge has roughly twice the intensity of the L_2 edge.

Next, there is the Coulomb interaction between the core-hole and the electrons in the d-shell. For example, there may now be Coulomb scattering between a $2p$ and a $3d$ electron as shown in Fig. 5. Let us consider the expression for the corresponding Coulomb matrix element (9). Here one of the indices ν_1 and ν_2 and one of the indices ν_3 and ν_4 must now refer to the $2p$ orbital and there are two possible combinations. If ν_2 and ν_3 refer to the $2p$ orbital we have

$$c^k(2,m_1;2,m_4)\; c^k(1,m_3;1,m_2) F^k(3,2;2,1).$$

The triangular condition for $c^k(1,m_3;1,m_2)$ requires $k\le 2$. Since only Y_{lm} with equal l and hence with equal parity are combined in one c^k only even k give non-vanishing contributions and we have two Coulomb integrals, $F^0(3,2;2,1)$ and $F^2(3,2;2,1)$.

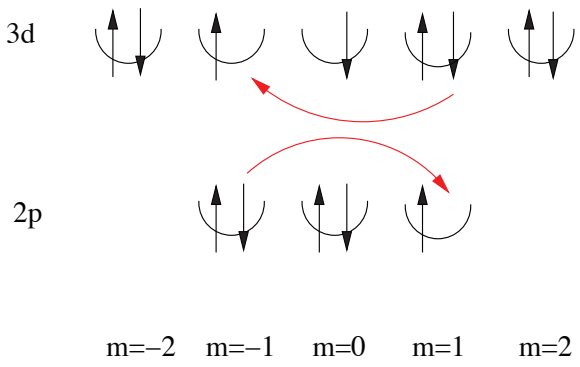

Fig. 5: *An electron in the $3d$ shell and an electron in the $2p$ shell scatter from one another.*

If ν_2 and ν_4 refer to the $2p$ orbital we have

$$c^k(2, m_1; 1, m_4)\ c^k(2, m_3; 1, m_2) G^k(3, 2; 2, 1).$$

The triangular condition for both c^k requires $k \leq 3$. Since now Y_{1m} and Y_{2m} are combined in one Gaunt coefficient only odd k contribute, so that we have two relevant exchange integrals, $G^1(3, 2; 2, 1)$ and $G^3(3, 2; 2, 1)$. Apart from these minor changes, the implementation of the d-p Coulomb interaction is exactly the same as the d-d interaction.

The Coulomb interaction between electrons in the $2p$ shell is definitely very strong – but it is irrelevant because we are considering only states with a *single hole* in this shell. Since this hole has no second hole to scatter from, the only effect of the Coulomb repulsion between electrons in the $2p$ shell is via the diagonal matrix elements which give a shift of the orbitals energy ϵ_{2p}. On the other hand ϵ_{2p} merely enters the position of the absorption edge, which would be $\approx \epsilon_{3d} - \epsilon_{2p}$ but not its spectral shape. Since we are not really interested in computing the onset of the edge, the precise value of ϵ_{2p} and hence the Coulomb interaction between $2p$ electrons is not important. Lastly we mention that the CEF effect on the inner-shell electrons is usually neglected.

Lastly, we discuss the dipole operator $D(\boldsymbol{n})$. This involves the matrix element of $\boldsymbol{n} \cdot \boldsymbol{r}$, where $\boldsymbol{n}$ is the vector which gives the polarization of the X-rays. This can be rewritten as

$$\boldsymbol{n} \cdot \boldsymbol{r} \ = \ r \sqrt{\frac{4\pi}{3}} \sum_{m=-1}^{1} \tilde{n}_m\ Y_{1,m}(\Theta, \phi)$$

where $\tilde{n}_1 = (-n_x + i n_y)/\sqrt{2}$, $\tilde{n}_0 = n_z$ and $\tilde{n}_{-1} = (n_x + i n_y)/\sqrt{2}$. It follows that

$$\begin{aligned} D(\boldsymbol{n}) &= \sum_{m,m'} \sum_{\sigma} d_{m,m'}\ c^\dagger_{3,2,m,\sigma} c_{2,1,m',\sigma} \\ d_{m,m'}(\boldsymbol{n}) &= d\ \tilde{n}_{m-m'}\ c^1(2, m; 1, m') \\ d &= \int_0^\infty dr\ r^3\ R_{3,2}(r) R_{2,1}(r). \end{aligned}$$

The factor of d merely scales the overall intensity of the spectrum and is largely irrelevant.

Combining all of the above one can compute X-ray absorption spectra. Fig. 6 shows examples

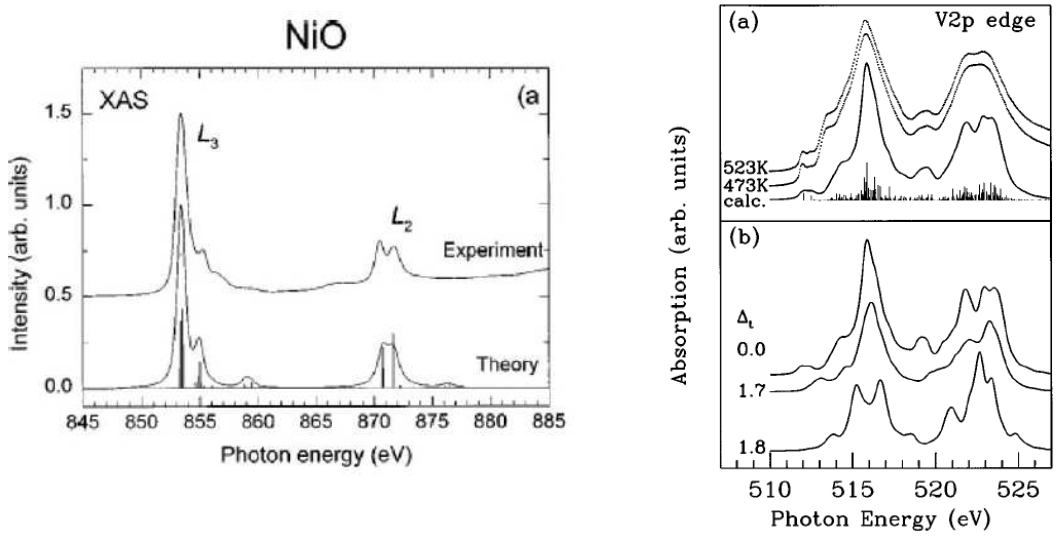

Fig. 6: *Comparison of experimental $2p$ XAS-spectra and results from cluster calculations: NiO (left) and $LiVO_2$ (right). The bottom part of the right-hand figure shows theoretical spectra calculated with different values of the CEF-strength Δ_t. Reprinted with permission from [19], Copyright 1999 and from [20], Copyright 1997 by the American Physical Society.*

from the literature where experimental $2p$-XAS spectra for NiO and $LiVO_2$ are compared to spectra obtained from multiplet theory. In both cases one can see the splitting of approximately 10-15 eV between the L_3 and L_2 edges. The edges do have an appreciable fine structure, however, and this is reproduced well by theory. The figure also illustrates the amount of information contained in XAS-spectra: the lower panel on the right hand side shows theoretical spectra calculated with different values of the CEF parameter, Δ_t. The strong difference between the spectra for $\Delta_t = 1.7$ and $\Delta_t = 1.8$ is due to a level crossing from a high-spin ground state of the Vanadium ion for $\Delta_t = 1.7$ to a low-spin ground state for $\Delta_t = 1.8$. In fact, $LiVO_2$ undergoes a phase transition at a temperature of ≈ 500 K whereby the magnetic susceptiblity drops almost to zero in the low temperature phase. A low-spin to high-spin transition of the Vanadium ion – for example caused by a change of the CEF due to thermal expansion – could be a possible explanation. It is obvious, however, that the spectrum for the low-spin ground state has no similarity whatsoever to the experimental spectrum at either 473 K or 523 K, rather these spectra a very similar to the spectrum of the high-spin ground state with $\Delta_t \approx 0$. A high-spin to low-spin transition therefore can be ruled out as the origin of the drop in magnetic susceptibility. This is one example how XAS can be used to determine the valence and spin of a given transition metal ion.

Let us discuss this in more detail. Photoelectron spectroscopies are often performed because for example the valence or the spin state of the transition metal ion in a given solid or molecule is unknown. Let us assume that we have two possible states of the ion, $|\Psi_0\rangle$ and $|\Psi_0'\rangle$, with energies E_0 and E_0' (for simplicity we assume that these are nondegenerate). Then we may ask: how will the spectrum change if we go from one ground state to the another? We note first that the final states $|\Psi_\nu\rangle$ and their energies E_ν in (21) and (22) are unchanged. What differs is first the energy

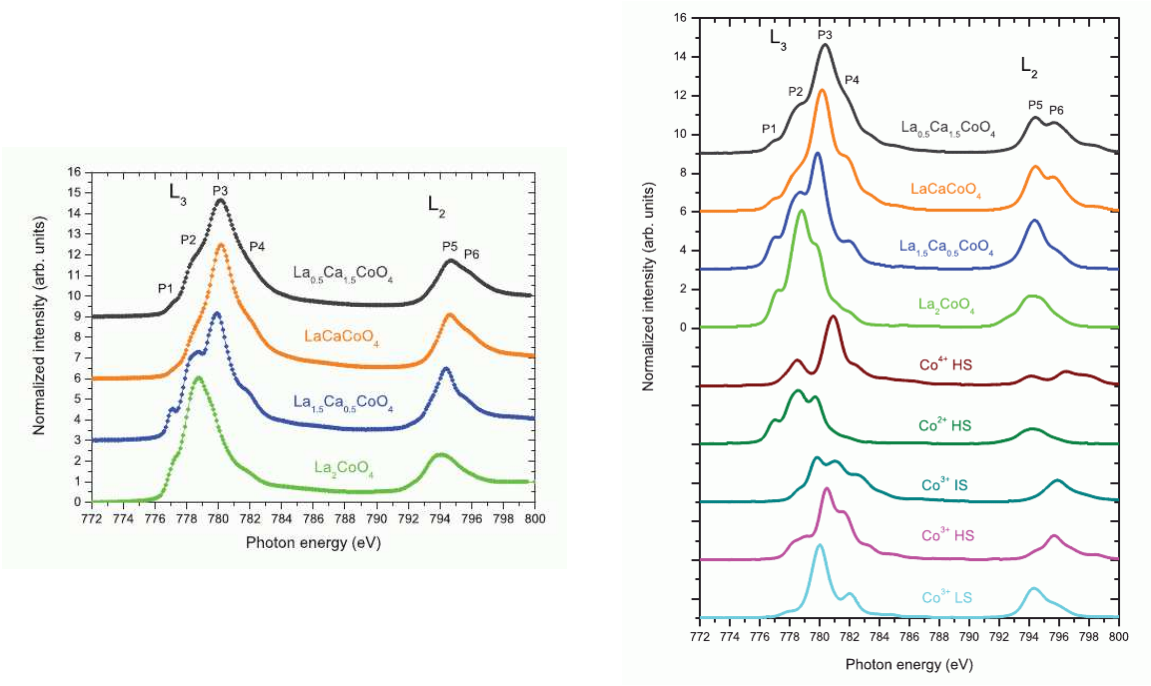

Fig. 7: *Left: Experimental Co 2p-XAS-Spectra for different Cobalt compounds with Perovskite structure. Right: The bottom part shows theoretical spectra calculated for different valence and spin states of Cobalt. By combining these spectra the actual experimental spectra can be reproduced almost quantitatively, see the four spectra at the top. Reprinted with permission from [21], Copyright 2011 by the American Physical Society.*

differences $E_\nu - E_0$. However, since we do not know E_0 and E_0' – otherwise we would know which one of them is lower in energy and hence the ground state – the absolute position of the peaks in the spectrum is of no significance. What is really relevant, however, is the *intensity* of the peaks which involves the matrix elements $|\langle\Psi_\nu|c|\Psi_0\rangle|^2$ or $|\langle\Psi_\nu|D(\boldsymbol{n})|\Psi_0\rangle|^2$. These matrix elements may change drastically when the ground state wave function $|\Psi_0\rangle$ changes and by comparing with cluster simulations the shape of the spectrum can give information about the valence and spin state of the transition metal ion. This is illustrated in Fig. 7, which shows experimental Cobalt $2p$ XAS-spectra of various Co-compounds with perovskite structure as well as theoretical spectra calculated by using the CTM4XAS package [10] for different valence and spin states of the Cobalt-ion. The experimental spectra obviously can be reproduced quite well by a superposition of such spectra for 'pure' valence and spin states of the Cobalt-ion. This implies that different Cobalt ions in the sample are in different valence and spin states whereby the percentages are simply given by the weight of the corresponding spectrum in the superposition.

To summarize this section: multiplet theory is of considerable importance in the interpretation of photoelectron spectroscopy. The simulated spectra usually show very good agreement with experimental ones. All of this shows that the multiplets of the free ion persist in the solid and that the proper desciption of the Coulomb interaction is crucial for the description of these compounds.

5 Conclusion

We have seen that the Coulomb repulsion between electrons in partially filled atomic shells leads to multiplet splitting. The simple estimate

$$E[d^n] \approx n \cdot \epsilon_d + U \cdot \frac{n(n-1)}{2}.$$

given in the introduction describes only the center of gravity of the energies of the d^n-derived states, and superimposed over this the Coulomb repulsion creates a multiplet spectrum with a width of several eV. While multiplet theory was derived originally for the discussion of spectroscopic data of atoms and ions in the gas phase, it has turned out that it is essential also for the understanding of many experiments on transition-metal compounds. Photoelectron spectroscopy, optical spectroscopy, electron spin resonance and inelastic neutron scattering all can be interpreted in terms of multiplets. The often excellent agreement between theory and experiment which can be obtained thereby is clear evidence that the multiplets of the free ion are a reality also in solids, with the only modification being some additional splitting due to CEF and modification of spectral intensities due to charge transfer. Any realistic description of $3d$ transition metal compounds therefore must take multiplet splitting into account.

Appendix

m	m'	c^0	$7\,c^2$	$21\,c^4$	a^0	$49\,a^2$	$441\,a^4$	b^0	$49\,b^2$	$441\,b^4$
±2	±2	1	-2	1	1	4	1	1	4	1
±2	±1	0	$\sqrt{6}$	$-\sqrt{5}$	1	-2	-4	0	6	5
±2	0	0	-2	$\sqrt{15}$	1	-4	6	0	4	15
±1	±1	1	1	-4	1	1	16	1	1	16
±1	0	0	1	$\sqrt{30}$	1	2	-24	0	1	30
0	0	1	2	6	1	4	26	1	4	36
±2	∓2	0	0	$\sqrt{70}$	1	4	1	0	0	70
±2	∓1	0	0	$-\sqrt{35}$	1	-2	-4	0	0	35
±1	∓1	0	$-\sqrt{6}$	$-\sqrt{40}$	1	1	16	0	6	40

Table 4: *The Gaunt coeficients* $c^k(2,m;2,m')$*, the coefficients* $a^k(2,m;2,m')$ *and* $b^k(2,m;2,m')$

m	m'	c^0	$15\,c^2$	$33\,c^4$	$\frac{429}{5}\,c^6$
±3	±3	1	-5	3	-1
±3	±2	0	5	$-\sqrt{30}$	$\sqrt{7}$
±3	±1	0	$\sqrt{10}$	$\sqrt{54}$	$-\sqrt{28}$
±3	0	0	0	$-\sqrt{63}$	$\sqrt{84}$
±2	±2	1	0	-7	6
±2	±1	0	$\sqrt{15}$	$\sqrt{32}$	$-\sqrt{105}$
±2	0	0	$-\sqrt{20}$	$-\sqrt{3}$	$4\sqrt{14}$
±1	±1	1	3	1	-15
±1	0	0	$\sqrt{2}$	$\sqrt{15}$	$5\sqrt{14}$
0	0	1	4	6	20
±3	∓3	0	0	0	$-\sqrt{924}$
±3	∓2	0	0	0	$\sqrt{462}$
±3	∓1	0	0	$\sqrt{42}$	$-\sqrt{210}$
±2	∓2	0	0	$\sqrt{70}$	$\sqrt{504}$
±2	∓1	0	0	$-\sqrt{14}$	$-\sqrt{378}$
±1	∓1	0	$-\sqrt{24}$	$-\sqrt{40}$	$-\sqrt{420}$

Table 5: *The Gaunt coeficients* $c^k(3,m;3,m')$

References

[1] J.H. de Boer and E.J.W. Verwey, Proc. Phys. Soc. London 49, 59 (1937)

[2] A.L. Fetter and J.D. Walecka: *Quantum Theory of Many Particle Systems* (McGraw-Hill, San Francisco, 1971)

[3] J.C. Slater: *Quantum Theory of Atomic Structure* (McGraw-Hill, New York, 1960)

[4] J.S. Griffith: *The Theory of Transition Metal Ions* (Cambridge University Press, Cambridge, 1961)

[5] L.D. Landau and E.M. Lifshitz: *Lehrbuch der Theoretischen Physik* (Akademie Verlag Berlin, 1988)

[6] E. Pavarini: The LDA+DMFT Approach, in [22]

[7] Yu. Ralchenko, A.E. Kramida, J. Reader, and NIST ASD Team (2011). NIST Atomic Spectra Database (ver. 4.1.0), `http://physics.nist.gov/asd`

[8] S. Sugano, Y. Tanabe, and H. Kitamura: *Multiplets of Transition Metal Ions* (Academic Press, New York 1970) (Dover, 1989)

[9] E. Koch: *The Lanczos Method*, in [22]

[10] See, e.g., the CTM4XAS package `http://www.anorg.chem.uu.nl/CTM4XAS`

[11] F.M.F. de Groot, J. of Electron Spectroscopy and Related Phenomena, **67** 525 (1994)

[12] F.M.F. de Groot, Coordination Chemistry Reviews, **249** 31 (2005)

[13] F.M.F. de Groot and A. Kotani: *Core Level Spectroscopy of Solids* (Taylor And Francis, 2008)

[14] C. Caroli, D. Lederer-Rozenblatt, B. Roulet, and D. Saint-James, Phys. Rev. B **8**, 4552 (1973)

[15] P.J. Feibelman and D.E. Eastman, Phys. Rev. B **10**, 4932 (1974)

[16] A. Fujimori and F. Minami, Phys. Rev. B **30**, 957 (1984)

[17] J. van Elp, J.L. Wieland, H. Eskes, P. Kuiper, G.A. Sawatzky, F.M.F. de Groot, and T.S. Turner, Phys. Rev. B **44**, 6090 (1991)

[18] A. Fujimori, N. Kimizuka, T. Akahane, T. Chiba, S. Kimura, F. Minami, K. Siratori, M. Taniguchi, S. Ogawa, and S. Suga, Phys. Rev. B **42**, 7580 (1990)

[19] M. Finazzi, N.B. Brookes, and F.M.F. de Groot, Phys. Rev. B **59**, 9933 (1999)

[20] H.F. Pen, L.H. Tjeng, E. Pellegrin, F.M.F. de Groot, G.A. Sawatzky, M.A. van Veenendaal, and C.T. Chen, Phys. Rev. B **55**, 15500 (1997)

[21] M. Merz, D. Fuchs, A. Assmann, S. Uebe, H. v.Löhneysen, P. Nagel, and S. Schuppler, Phys. Rev. B **84**, 014436 (2011)

[22] E. Pavarini, E. Koch, D. Vollhardt, and A. Lichtenstein (eds.):
The LDA+DMFT approach to strongly correlated materials,
Reihe Modeling and Simulation, Vol. 1 (Forschungszentrum Jülich, 2011)
`http://www.cond-mat.de/events/correl11`